DOI: 10.24996/ijs.2023.64.4.15

ISSN: 0067-2904

Synthesis and Investigation of the Structural Characteristics of Zinc Oxide Nanoparticles Produced by an Atmospheric Plasma Jet

Kadhim A. Aadim, Ibrahim K. Abbas*

Department of Physics, College of Science, University of Baghdad, Baghdad, Iraq

Received: 12/5/2022 Accepted: 13/8/2022 Published: 30/4/2023

Abstract

In this paper, ZnO NPs were prepared using D.C high-voltage and high frequency with an output of 6 kHz at two different preparation times preparation (10,12) minutes. Transmission electron microscopy (TEM) with (FE-SEM) was used to examine the homogenous, compact, and dense surface of the zinc oxide nanoparticles created with apparent grain size determined by (XRD), XRD results explain that the increase of the preparation time from 10 minutes to 12-minute caused an increase in crystallite size. In addition, FE-SEM showed that the increase in the ZnO NPs cluster distribution with particle size increases with increasing the preparation time. AFM was also utilized to determine the degree of cooperation between the surfaces of the zinc oxide nanoparticles, with having a high degree of stability by zeta potential -13.3±1.8mV at 12 minutes.

Keywords: FE-SEM Plasma, Zinc oxide nanoparticles AFM, Zinc oxide nanoparticles, Plasma Jet, TEM ZnO NPs, ZnO NPs Zeta Potential.

تحضير والتحقق للخصائص التركيبية لجسيمات أوكسيد الزنك النانوية المنتجة بواسطة بلازما النفث عند الضغط الجوي

كاظم عبد الواحد عادم، إبراهيم كريم عباس*

قسم الفيزياء، كلية العلوم، جامعة بغداد، بغداد، العراق

الخلاصة

في هذا البحث تم تحضير ZnO NPs باستخدام مجهز قدرة عالي الجهد مع تردد خرج 6 كيلو هرتز عند زمنين مختلفين للتحضير (10، 12) دقيقة. تم استخدام المجهر الإلكتروني النافذ مع الميكروسكوب الالكتروني الماسح لفحص السطح المتجانس والكثيف لجسيمات أوكسيد الزنك النانوية التي تم تخليقها باستخدام منظومة البلازما غير الحرارية، حيث اظهر حيود الأشعة السينية لجسيمات أوكسيد الزنك النانوية عدداً من القمم مع حجم حبيبات ظاهر ومحدد، توضح نتائج XRD أن وقت التحضير المتزايد من 10 – 12 دقيقة تسبب في زيادة حجم البلورات النانوية. بالإضافة إلى ذلك، أظهر FE–SEM أن الزيادة في توزيع كتلة ZnO NPs مع حجم الجسيمات تزداد مع زيادة وقت التحضير. تم استخدام AFMأيضًا لتحديد درجة

*Email: ibrahim.kareem1104a@sc.uobaghdad.edu.iq

التجانس بين أسطح جسيمات أوكسيد الزنك النانوية المحضرة، وأظهرت النتائج وجود درجة عالية من الثبات بواسطة إمكانات زيتا −13.3 ± 1.8 مللي فولت في 12 دقيقة.

1. Introduction

Zinc nanoparticles are microscopic particles whose diameter is smaller than 100 nm[1]. Despite their small size, they have large surface area compared to their weight[2]. Zinc oxide nanoparticles have a wide range of physical and chemical characteristics depending on how they are manufactured[3]. These include laser ablation, plasma jets, hydrothermal techniques, electrochemical depositions, chemical vapor depositions, and thermal decompositions of ZnO nanoparticles[4]. Zinc oxide nanoparticles made out of zinc oxide are among the most studied since they are used in many different applications[5]. Zinc oxide nanoparticles, the second most common metal oxide after iron, are cheap, safe, and simple to make[6]. Changing the shape of the zinc oxide nanoparticles and utilizing alternative synthesis techniques, precursors, or materials can readily alter their physical and chemical properties[7]. Zinc oxide nanoparticles are insoluble in water [1]. The use of atmospheric pressure plasmas in a wide range of applications in the biological, nanotechnology, and agricultural fields has recently piqued interest[8], which is particularly true in the biomedical field, where applications include bacteria inhibition, tissue regeneration, and dental bleaching[9]. Research into the properties of atmospheric plasma processes to determine whether they can be used for nanoparticle preparation, sterilization, and disinfection treatment, as well as for protecting industrial materials, equipment, and electronics from biological damage and microbiologically induced corrosion, has become increasingly important in recent years[10,11]. Plasma treatment of living tissues produces the desired therapeutic effect in the sterilization and bleeding arrest, bleeding control, and cure of certain skin diseases, among other applications[2]. As a result of the increasing need from mankind for new high-productivity sterilization and disinfection technologies that do not require high temperatures and are simple to operate, this trend has taken on a significant amount of significance in recent years[10]. As a result of their distinct features compared to their bulk equivalents, nanomaterials have attracted a significant attention in recent years[12]. Nanomaterials, which are incredibly small in size and have a large surface area, have demonstrated significant biological activity in the human body[13]. Nanomaterials are essential in the field of biomedicine[13,14]. Despite this, our present understanding of nanomaterials' behavior concerning human health is still insufficient[15]. As a result, developing a toxic-chemical-free synthesis method is critical for the advancing of nanotechnology for biomedical applications[16]. Due to its distinctive characteristics compared to solid, liquid, and gas-phase synthesis methodologies, plasma technology is currently getting significant interest as a prominent "green" synthesis method for nanomaterials[7]. Non-thermal plasma has the potential to kill cancer cells either directly or indirectly[17]. Increased specificity and efficiency of the treatment can be achieved using conjugated or unconjugated NPs[18]. There have been numerous studies in which researchers have used antibody-conjugated nanoparticles (NPs) to increase cell death and decrease the viability of cancer cells[19]. Zinc oxide nanoparticles are also recognized for their low toxicity and excellent UV-absorption, making them a suitable candidate to be employed in the biomedical area[16]. ZnO NPs are suitable for use in ceramics and biomedicine due to their capacity to act as a good surface material because of their strong and stiff structure[20]. ZnO NPs are naturally recognized as highly resistant to microorganisms[7]. Because of this, they are widely employed in biomarking, biosensing, medication delivery, gene delivery, and nanomedicine[21]. ZnO NPs are soluble in an acidic environment, making them a good candidate for use as a multifunctional nanocarrier for easing the delivery and release of pharmaceuticals[22]. These characteristics provide a great opportunity to develop nanomaterials as effective antimicrobial

agents in the future[23]. One of the most intriguing of these is nanostructured zinc, which has a significant antibacterial activity while having high thermal stability and being quite inexpensive[24].

The aim of this article is through the use of a constant flow of argon gas 3 *l/min* to generate non-thermal plasma, through which ZnO NPs are prepared and synthesized, and also to study the structure of ZnO NPs prepared at different times

.

2. Experimental Setup

2.1. Preparation of Atmospheric Plasma Jet System

Figure 1 represents the non-thermal plasma operating system at atmospheric pressure with an enlarged small image inside the figure showing the tip of the plasma jet, through which argon gas flows out and interacts with distilled water. A zinc sheet was immersed in the beaker (a 99.99 percent pure zinc sheet purchased from British drug LTD/London). The system has a high voltage power supply of up to 25 kV with a cut-off frequency of 150 kHz. The plasma needle was made of stainless steel with an inner diameter of 3mm; it represents the cathode electrode. The anode electrode was connected to a zinc sheet. The argon gas was used to generate plasma. To prepare ZnO NPs, argon gas was used to generate plasma. The amount of argon gas coming out was controlled by a control unit called flow meter.

2.1.A. Argon Gas Flowmeter

It is an instrument that is used to indicate the amount of argon gas moving through a pipe or conduit, where the flow device contains an argon gas inlet that is connected to the argon gas bottle directly. The device also has a gas exit that is connected with the plasma needle through a connecting tube, the amount of argon gas passing towards the plasma needle is controlled through a graduated control unit.

2.1.B. High Voltage Power Supply

The high voltage power supply is laboratory built and manufactured to generate high voltages ranging from 1 to 25 kV with a frequency up to 150 kHz. The high voltage power supply is 220 volts alternating voltage, representing the entry voltage (input). The high voltage from the power supply is controlled through an electrical control circuit. The applied voltage (output) to generate the non-thermal plasma and synthesize the zinc oxide nanoparticles was fixed at 21 kV. The cathode of the high voltage power supply was connected to the stainless-steel needle. The anode electrode was connected to the zinc sheet (the part not in the distilled water) used to generate the nanoparticles. Figure 2 shows a schematic diagram of the experimental setup.

2.2. Zinc Oxide Nanoparticles Preparation

In this experiment, a (7x1) cm^2 high-purity zinc sheet was used, and a zinc metal sheet was placed in a 10 ml beaker filled with distilled water. The argon gas was passed through the plasma needle, which was fixed perpendicular to the beaker where the zinc sheet was placed with distilled water. The gas molecules interact with the distilled water in the beaker, causing a series of reactions with the metal surface, which results in a change in color of the distilled water to another color, which is as close to light white, indicating the formation of nanoparticles of this metal, as shown in Figure 2. ZnO NPs were prepared using a fixed argon gas flow of 3 *l/min* and a voltage of 21 kV at various times (10, 12) minutes. Consequently, the structural characteristics of the zinc oxide nanoparticles formed at these two times was studied. The length of the plasma plume was 3.6 cm, with each experiment being repeated three times to ensure the accuracy of the data. The characterization of the produced ZnO NPs was carried out in Iran at the University of Kashan for XRD (Phillips PANalytical X'PERT,

Holland), FE-SEM, EDX (TESCN MIRA3, French), and TEM, with Zeta Potential (HORBIA Scientific SZ-100, Poland).

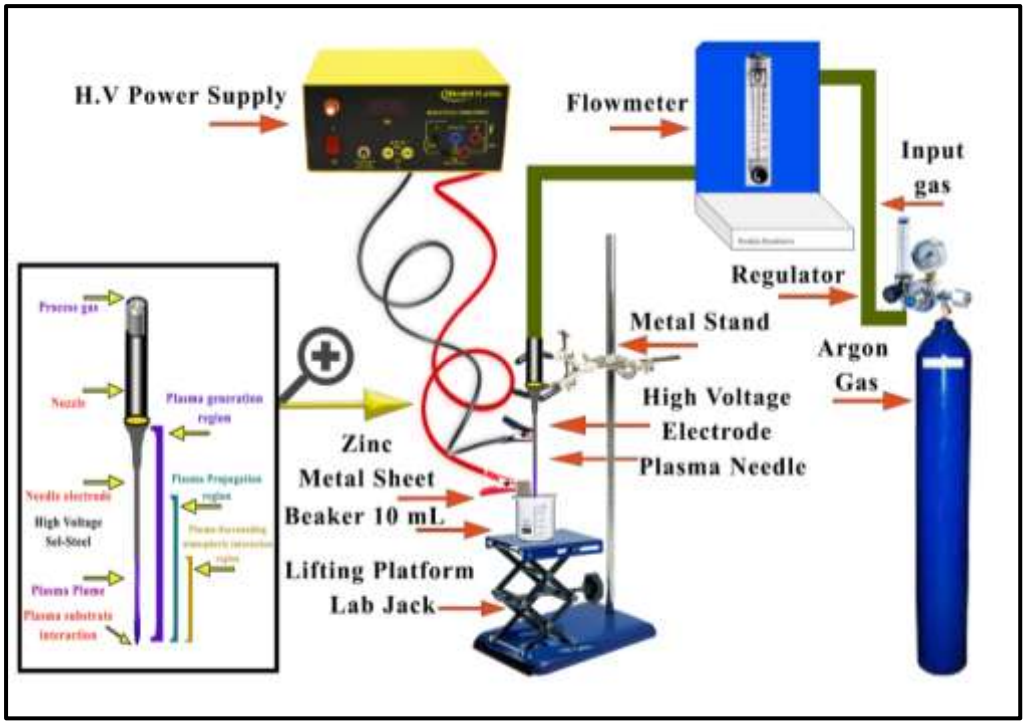

Figure 1: Schematic diagram of atmospheric plasma jet experimental setup for the synthesis of zinc oxide nanoparticles.

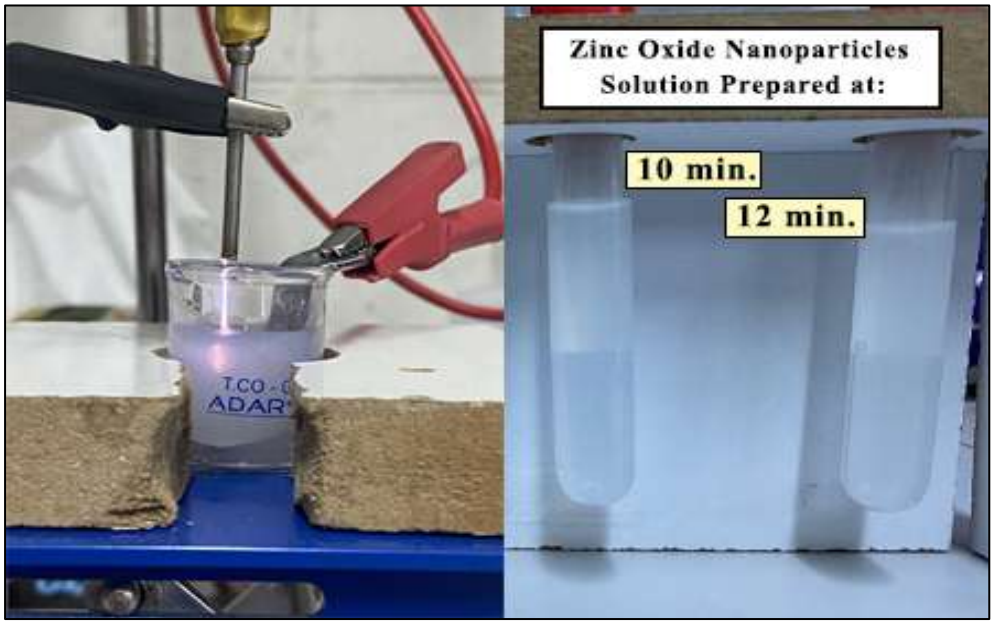

Figure 2: Synthesis of zinc oxide nanoparticles by atmospheric plasma jet at (10 and 12) minutes.

3. Results and Discussion

3.1. Investigation of the ZnO NPs Crystal Structure

Figure 3 shows the XRD spectra of ZnO NPs, which are in agreement with the spectrum of zinc oxide reference (JCPDS code no. 36-1451). It demonstrates that the produced nanoparticles have a hexagonal structure with excellent purity, with the appearance of several

different peaks at 2θ° = (31.77°), (34.65°), (36.25°), (47.53°), (57.26°), (62.90°), and (68.16°) corresponding to (100), (002), (101), (102), (110), (103), and (112), respectively. It depicts the phase of pure zinc metal after it has been prepared by plasma in the distilled water for (10, 12) min. The XRD spectrum apparent peaks imply that it is in line with previous research and literature that has sought to synthesize zinc oxide nanoparticles[25,26]. The newly generated nanoparticles have a crystallite size of 29.136 nm at 10 minutes and 31.159 nm for 12 minutes. The highest peak is the one corresponding to the (100) plane. As the particle size grows, the peak intensity increases. It can be noted that the size of nanoparticles at the 12 min time is slightly larger than that at 10 min time. Thus increasing the variance of the properties of these nanoparticles, consequently, the diameters of these formed nanoparticles increased slightly and notably, as can be seen from the XRD patterns. The difference between the spectrum at the first time 10 minutes and the spectrum at the second time 12 minutes, is the increase in all the peaks intensity in 12 min, and here the effect of preparation time appears significantly on the size of the zinc nanoparticles formed, as the size of the prepared nanoparticles increased. The particle size was 29.136 nm at 10 minutes and 31.159 nm for 12 minutes. Due to faults in stacking, a smaller coherent scattering region (100) may be observed along or at the top (100) than in other directions, as shown by high-resolution TEM pictures of zinc oxide nanoparticles.

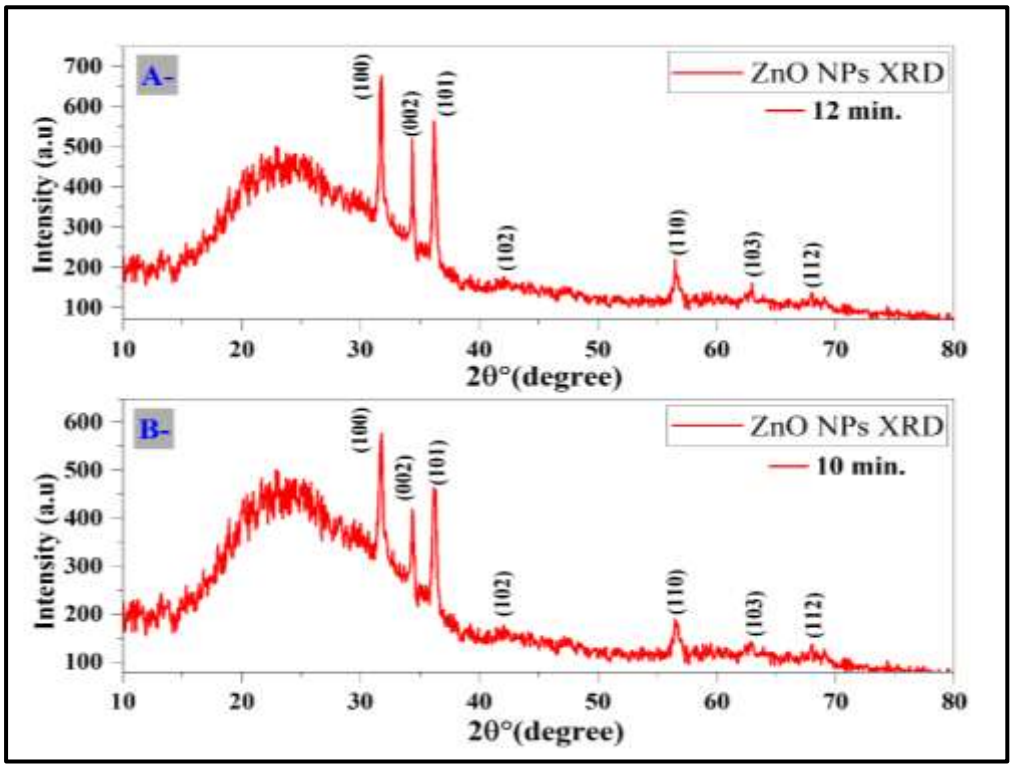

Figure 3: XRD patterns of zinc oxide nanoparticles prepared by APJS at (10, 12) minutes.

3.2. Atomic Force Microscope of Zinc Oxide Nanoparticles

Clusters with consistent sizes and symmetrical forms of ZnO NPs are formed when gas molecules exiting the plasma nozzle come into the beaker and contact the zinc metal plate immersed in the solution, as shown in Figure 4 and Figure 5. As can be seen in the figures, the formation of cubes and nanorod-like structures was accompanied by the formation of some spherical zinc oxide nanoparticles. The average diameter of the nanorods was 22.45 nm, and the average particle size was 5.17 nm, with roughness being 3.071 nm in 12 minutes. Whereas, for the 10 minutes time, the average diameter was 21.11 nm, average particle size 4.63 nm, and roughness 2.953. The histogram of the mean value of particle size distribution

shows that it ranged from 23.5 to 32 nm in the 10 minutes time, and from 22 to 30 nm in the 12 minutes time.

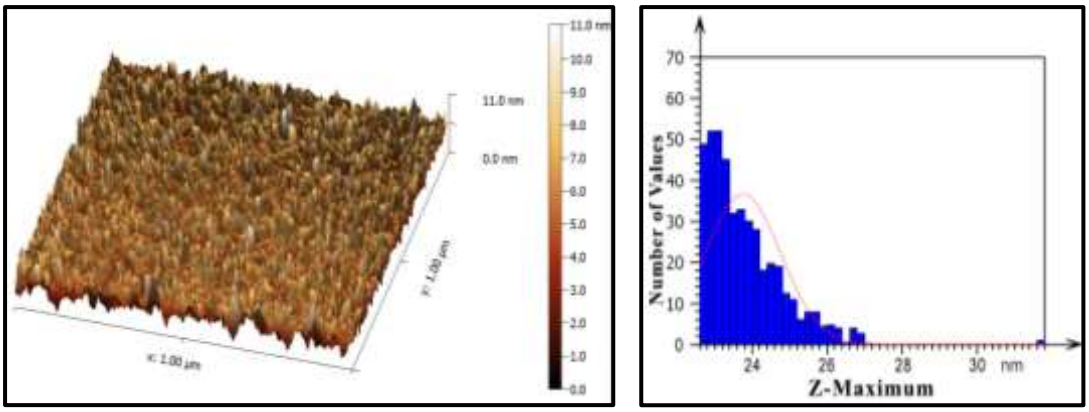

Figure 4: AFM image for zinc oxide nanoparticles and histogram prepared by atmospheric plasma jet at 10 minutes**.**

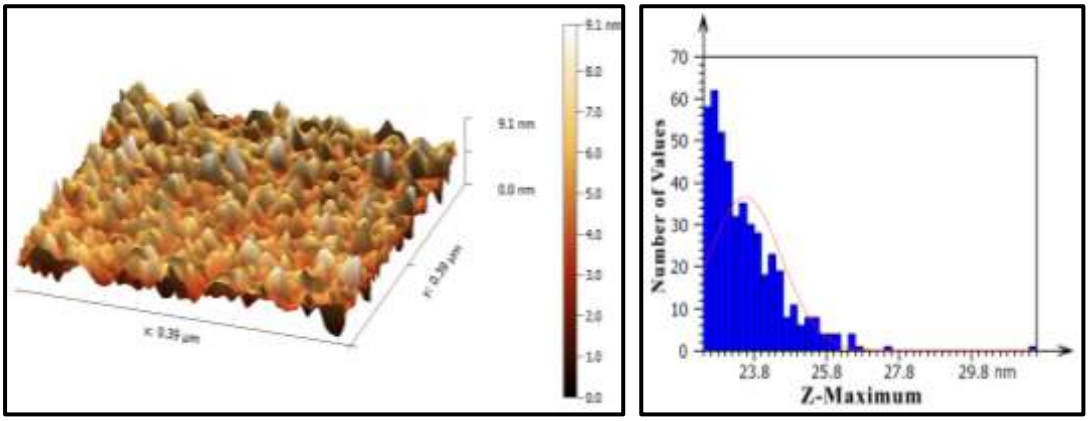

Figure 5: AFM image for zinc oxide nanoparticles and histogram prepared by atmospheric plasma jet at 12 minutes.

3.3. Surface Morphological Investigation and TEM of ZnO NPs

It can be seen from the FE-SEM images of both preparation times and the zoom view (Figure 6 and Figure 7) that the nanostructure of the prepared zinc oxide nanoparticles is relatively symmetric and some are identical in shape; these nanospheres appear as flowers white and black. It can clearly be seen that the zinc oxide nanoparticles do not have a fixed shape and their distribution is obvious, but in turn, the solution of ZnO NPs synthesized in both preparation times (10, 12) minutes becomes oxidized material clustering and growing irregularly in shape. This is clear from these images showing the formation of zinc oxide nanoparticles in the first and second time. This demonstrates that the nanoparticles were homogeneous throughout the process. The surface morphology of zinc oxide nanoparticles produced by plasma jet was determined using FE-SEM. Figure 8 displays the EDX spectra that are closely related to this created zinc oxide nanoparticle sample. Increasing the nanoparticles preparation time enables the production of exceedingly tiny structures from the element's nanoparticles. This results is consistent with previous studies [6,27]. Other elements, such as carbon and oxygen, were detected in the EDX spectra of ZnO NPs in addition to zinc, the presence of these elements is almost certainly due to contamination from the glass substrate and SEM chamber or solution in beaker, as all of these elements play a role in the process of forming ZnO NPs during their interaction with liquid at the nozzle of the plasma jet. The results are in good agreement with the XRD results.

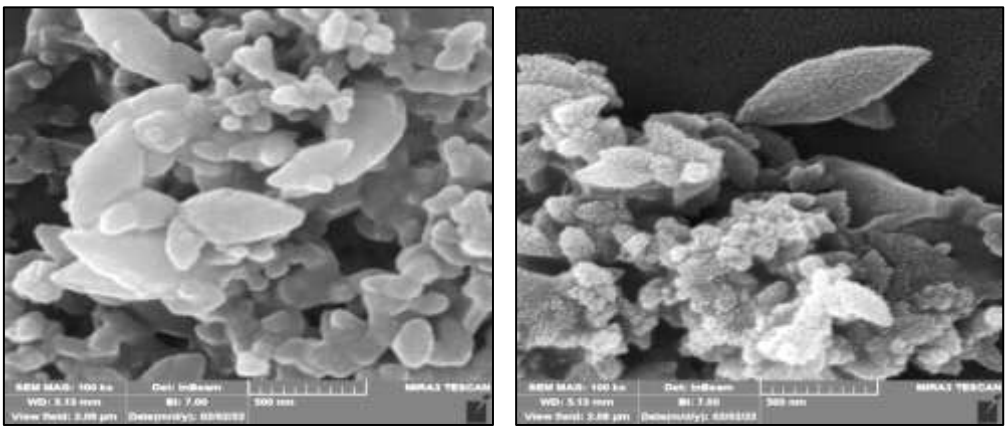

Figure 6: FE-SEM Images of Zinc Oxide Nanoparticles Prepared by APJS at 10 minutes.

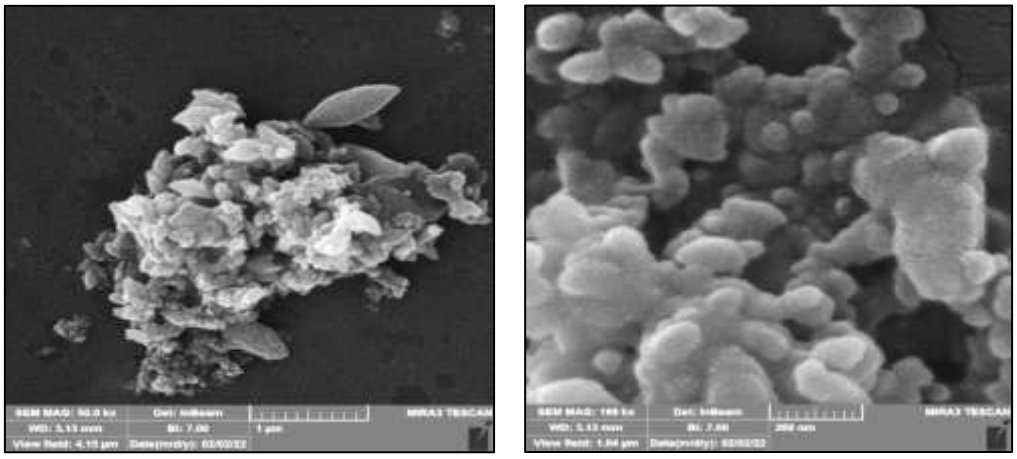

Figure 7: FE-SEM images of zinc oxide nanoparticles prepared by APJS at 12 minutes.

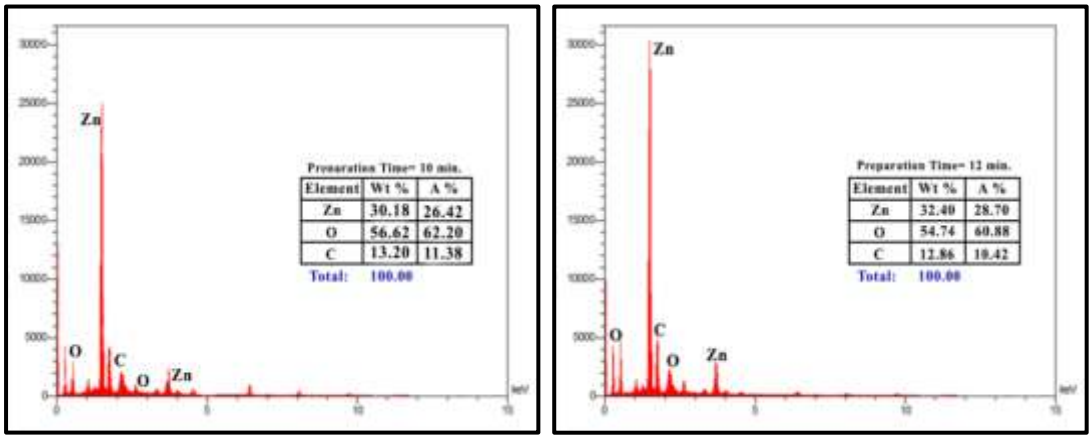

Figure 8: EDX spectrum of zinc oxide nanoparticles and elements percentage in atomic weight at (10, 12) minutes

TEM images of ZnO NPs at scales of 150 nm and 300 nm are shown in Figure 9. It is clear that the development of scattered spherical nanoparticles is analogous to the construction of an interconnected grid of atoms and molecules, and the presence of some large particles represents the bonding and agglomeration of these ZnO NPs. The particle size of ZnO NPs is an important physical factor that influences the fate of using ZnO NPs in a variety of many fields. This results of TEM images is consistent with prior findings[28,29]. When the properties of the formed nanoparticles are compared to the XRD results, one can

find that the values obtained are in good agreement with the results obtained from the TEM image in both preparation times.

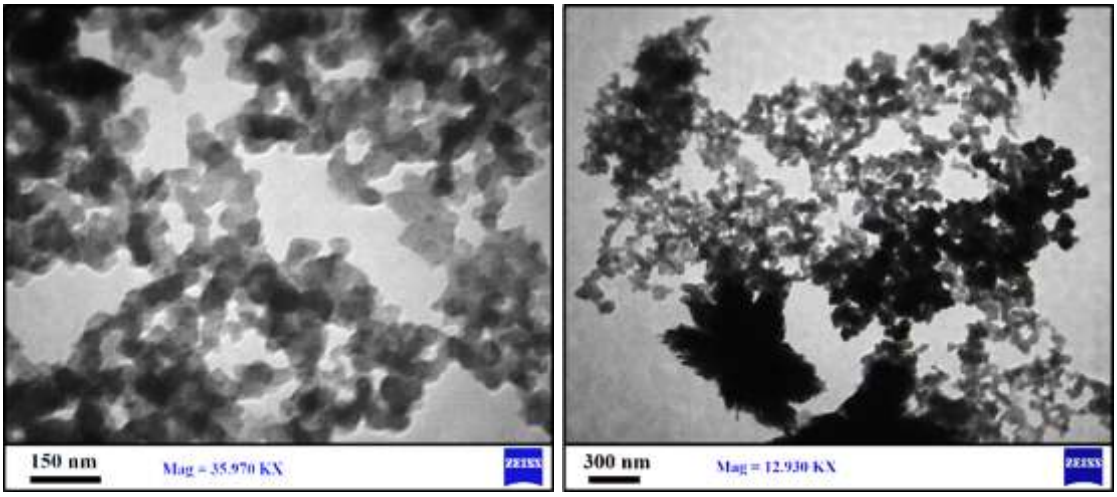

Figure 9: TEM image of zinc oxide nanoparticles prepared by plasma jet scaled at 150 nm and 300 nm for (10, 12) minutes.

3.4. Zeta Potential (ZP) of Zinc Oxide Nanoparticles

Figure 10 shows the zeta-potential of zinc oxide nanoparticles prepared by plasma jet at 10 minutes and 12 minutes. Where measurements have Zeta potential (ZP) values of -12.6±1.2 mV and -13.3±1.8 mV, respectively, indicating high degree of stability. The high values of ZP mean that the synthesized ZnO NPs are highly charged particles and will prevent the aggregation and agglomeration due to their large repulsion force. The nanoparticles with ZP of -12.6±1.2 mV indicates that they have little less dispersion which lead to particles aggregation and/or agglomeration, coagulation, or flocculation due to Van der Waals attraction force, whereas ZnO NPs with ZP -13.3±1.8 mV are considered of better colloidal stability condition. The origin of particles agglomeration is the high free surface energy and the large surface area of the nanoparticles. This agrees with prior findings[30,31].

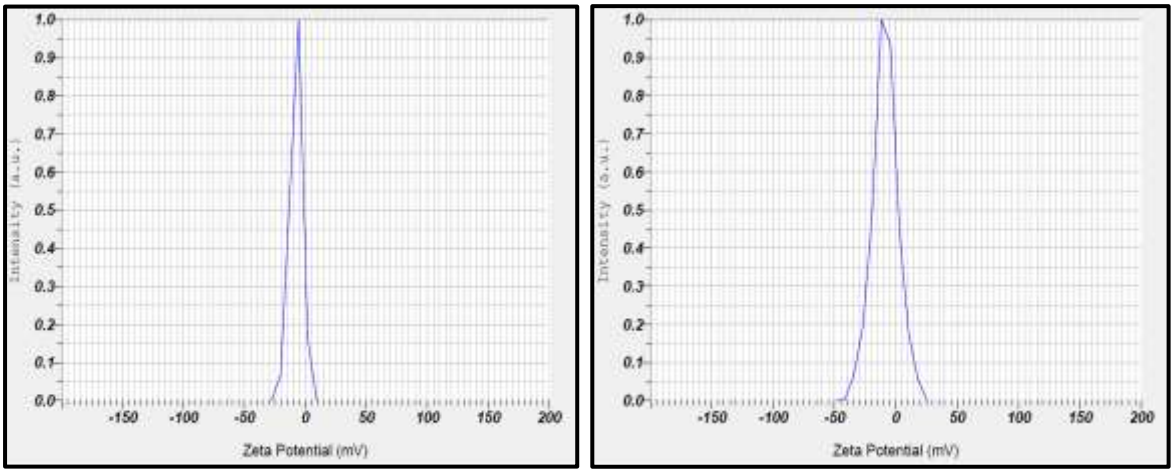

Figure 10: Zeta potential of zinc oxide nanoparticles prepared by atmospheric plasma jet at (10, 12) minutes.

4. Conclusion

There was a distinct effect of preparation time (10, 12) minutes on zinc oxide nanoparticles that were prepared by atmospheric plasma jet. Several peaks appeared in the XRD patterns. The images of FE-SEM and TEM for both preparation times (10, 12) minutes indicated high homogeneity and morphological of ZnO NPs synthesized. The results explain that increasing the preparation time from 10 minutes to 12 minutes caused an increase in the particle size and average diameter of zinc oxide nanoparticles. The diameter of the zinc oxide nanoparticles was about 22.45 nm as shown in AFM at 12 minutes whereas it was 21.11 nm at 10 minutes. The in EDX results showed the presence of oxygen and carbon in different concentrations in (10, 12) minutes, with a high stability of zeta potential -13.3±1.8 mV in 12 minutes and -12.6±1.2 mV in 10 minutes.

Acknowledgement

We would like to express gratitude and grateful thanks and deeply extend thanks to the plasma laboratory in physics department-college of sciences/Baghdad University. And finally, we offer gratitude to everyone who gave us the inspiration to continue the thorough knowledge path.

References

[1] H. Y. Sohn and A. Murali, "Plasma Synthesis of Advanced Metal Oxide Nanoparticles," a review," *Molecules*, vol 26, no. 5, p. 1456, 2021.

[2] A. Nikiforov, X. Deng, Q. Xiong, U. Cvelbar, N. DeGeyter, R Morent and C. Leys., "Non-thermal plasma technology for the development of antimicrobial surfaces: a review," *J. Phys. D. Appl. Phys.*, vol. 49, no. 20, p. 204002, 2016.

[3] K. A. Aadim and R. H. Jassim, "Determination of plasma parameters and nanomaterial's synthesis of Zn and Mn using laser induced plasma spectroscopy," in *AIP Conference Proceedings*, vol. 2372, no. 1, p. 80014, 2021.

[4] M. Cierech, J. Wojnarowicz, A. Kolenda , A. Krawczyk-Balska , E. Prochwicz, B. Woźniak, W. Łojkowski , E. Mierzwińska-Nastalska "Zinc oxide nanoparticles cytotoxicity and release from newly formed PMMA–ZnO nanocomposites designed for denture bases," *Nanomaterials*, vol. 9, no. 9, p. 1318, 2019.

[5] S.-E. Jin and H.-E. Jin, "Synthesis, characterization, and three-dimensional structure generation of zinc oxide-based nanomedicine for biomedical applications," *Pharmaceutics*, vol. 11, no. 11, p. 575, 2019.

[6] S. Fakhari, M. Jamzad, and H. Kabiri Fard, "Green synthesis of zinc oxide nanoparticles: a comparison," *Green Chem. Lett. Rev.*, vol. 12, no. 1, pp. 19–24, 2019.

[7] M. Bandeira, M. Giovanela, M. Roesch-Ely, D. M. Devine, and J. da Silva Crespo, "Green synthesis of zinc oxide nanoparticles: A review of the synthesis methodology and mechanism of formation," *Sustain. Chem. Pharm.*, vol. 15, p. 100223, 2020.

[8] R. S. Mohammed, K. A. Aadim, and K. A. Ahmed, "Estimation of plasma parameters in a DC atmospheric pressure Argon plasma jet," in *AIP Conference Proceedings*, vol. 2386, no. 1, p. 80050, 2022.

[9] K. A. Aadim and H. R. Najem, "Effect of cold atmospheric pressure plasma needle on DNA." *J. Appl. Phys.*, vol. 7, no. 6, pp. 52-55, 2015.

[10] M. Laroussi, "Low-temperature plasmas for medicine?," *IEEE Trans. plasma Sci.*, vol. 37, no. 6, pp. 714–725, 2009.

[11] I. Adamovich, S. D. Baalrud, A. Bogaerts, P. J. Bruggeman, M. Cappelli, V. Colombo, "The 2017 Plasma Roadmap: Low temperature plasma science and technology," *J. Phys. D. Appl. Phys.*, vol. 50, no. 32, 2017, doi: 10.1088/1361-6463/aa76f5.

[12] K. S. Kim and T. H. Kim, "Nanofabrication by thermal plasma jets: From nanoparticles to low-dimensional nanomaterials," *J. Appl. Phys.*, vol. 125, no. 7, p. 70901, 2019.

[13] G. Ciofani, *Smart nanoparticles for biomedicine*. Elsevier, 2018.

[14] W. Q. Lim and Z. Gao, "Plasmonic nanoparticles in biomedicine," *Nano Today*, vol. 11, no. 2, pp. 168–188, 2016.

[15] O. Gherasim, R. A. Puiu, A. C. Bîrcă, A.-C. Burduşel, and A. M. Grumezescu, "An updated review on silver nanoparticles in biomedicine," *Nanomaterials*, vol. 10, no. 11, p. 2318, 2020.

[16] G. V. Vimbela, S. M. Ngo, C. Fraze, L. Yang, and D. A. Stout, "Antibacterial properties and toxicity from metallic nanomaterials," *Int. J. Nanomedicine*, vol. 12, pp. 3941–3965, 2017, doi: 10.2147/IJN.S134526.

[17] R. Shrestha, D. P. Subedi, J. P. Gurung, and C. S. Wong, "Generation, characterization and application of atmospheric pressure plasma jet," *Sains Malaysiana*, vol. 45, no. 11, pp. 1689–1696, 2016.

[18] P. Biswas and C.-Y. Wu, "Nanoparticles and the environment," *J. Air Waste Manage. Assoc.*, vol. 55, no. 6, pp. 708–746, 2005.

[19] S. Mitra, L. N. Nguyen, M. Akter, G. Park, E. H. Choi, and N. K. Kaushik, "Impact of ROS generated by chemical, physical, and plasma techniques on cancer attenuation," *Cancers (Basel).*, vol. 11, no. 7, p. 1030, 2019.

[20] Y. Xie, Y. He, P. L. Irwin, T. Jin, and X. Shi, "Antibacterial activity and mechanism of action of zinc oxide nanoparticles against Campylobacter jejuni," *Appl. Environ. Microbiol.*, vol. 77, no. 7, pp. 2325–2331, 2011, doi: 10.1128/AEM.02149-10.

[21] S. Kavitha, M. Dhamodaran, R. Prasad, and M. Ganesan, "Synthesis and characterisation of zinc oxide nanoparticles using terpenoid fractions of Andrographis paniculata leaves," *Int. Nano Lett.*, vol. 7, no. 2, pp. 141–147, 2017, doi: 10.1007/s40089-017-0207-1.

[22] S. V. Gudkov, D. E. Burmistrov, D. A. Serov, M. B. Rebezov, A. A. Semenova, and A. B. Lisitsyn, "A Mini Review of Antibacterial Properties of ZnO Nanoparticles," *Front. Phys.*, vol. 9, article 641481, pp. 1–12, 2021, doi: 10.3389/fphy.2021.641481.

[23] K. S. Khashan, G. M. Sulaiman, and S. A. Hussain, "Synthesis and Characterization of Aluminum Doped Zinc Oxide Nanostructures by Nd: YAG Laser in Liquid," *Iraqi J. Sci.*, vol. 61, no. 10, pp. 2590–2598, 2020.

[24] H. Sturikova, O. Krystofova, D. Huska, and V. Adam, "Zinc, zinc nanoparticles and plants," *J. Hazard. Mater.*, vol. 349, pp. 101–110, 2018.

[25] S. S. Kumar, P. Venkateswarlu, V. R. Rao, and G. N. Rao, "Synthesis, characterization and optical properties of zinc oxide nanoparticles," *Int. Nano Lett.*, vol. 3, article no. 30, pp. 1–6, 2013.

[26] R. Marsalek, "Particle Size and Zeta Potential of ZnO," *APCBEE Procedia*, vol. 9, pp. 13–17, 2014, doi: 10.1016/j.apcbee.2014.01.003.

[27] H. Nikiyan, O. Davydova, and D. Senatorova, "Morphology and biological activity of Co and Zn oxide nanoparticles and ferrates," in *Chemical Physics of Molecules and Polyfunctional Materials*, Orenburg State University 2021, pp. 70–73.

[28] M. I. Din, S. Jabbar, J. Najeeb , R. Khalid , T. Ghaffar, M. Arshad, S. A Khan , S. Ali "Green synthesis of zinc ferrite nanoparticles for photocatalysis of methylene blue," *Int. J. Phytoremediation*, vol. 22, no. 13, pp. 1440–1447, 2020.

[29] T. Gur, I. Meydan, H. Seckin, M. Bekmezci, and F. Sen, "Green synthesis, characterization and bioactivity of biogenic zinc oxide nanoparticles," *Environ. Res.*, vol. 204, part A, p. 111897, 2022.

[30] M. H. Hidayat Chai, N. Amir, N. Yahya, and I. M. Saaid, "Characterization and Colloidal Stability of Surface Modified Zinc Oxide Nanoparticle," *J. Phys. Conf. Ser.*, vol. 1123, no. 1, p. 012007, 2018, doi: 10.1088/1742-6596/1123/1/012007.

[31] D. K. Naser, A. K. Abbas, and K. A. Aadim, "Zeta potential of Ag, Cu, ZnO, CdO and Sn nanoparticles prepared by pulse laser ablation in liquid environment," *Iraqi J. Sci.*, vol. 61, no. 10, pp. 2570–2581, 2020, doi: 10.24996/ijs.2020.61.10.13.